

## UA9 report for 2009

### Introduction

In a hadron collider, such as the LHC, a two-stages collimation system is used to absorb the beam halo in view of preventing damages of the accelerator components and reducing the background in the experimental apparatus. The halo particles repeatedly interact with the primary collimator and are eventually deflected by multiple Coulomb scattering towards the secondary bulk absorber. The halo generation is a rather complex process induced by non-linear components of the guiding fields, power supplies ripple and synchrotron motion resulting in a diffusive growth of the oscillation amplitude of the particles at the edge of the beam core. The per-turn amplitude increase resulting from the joint effect of diffusion and Coulomb scattering is, in general, very small (smaller than 1  $\mu\text{m}$ ). In these conditions a fraction of the halo particles will collide very close to the edge of the collimators and have a finite probability of being back scattered, eventually producing loss in the sensitive areas of the accelerator. Tertiary collimators are used to mitigate this damage. However diffractive protons produced at a small grazing angle are less easily intercepted.

Bent crystals used as primary collimators should deflect the incoming halo particles very deeply onto the absorber far from its edge (see Fig.1), thereby improving the collimation efficiency even at very small impact parameters. At the same time the rate of the diffractive events produced during the channeling process is expected to decrease dramatically. The particle trajectories, which cross the crystallographic planes at small angles, are governed by the crystal potential averaged along the planes [1]. Below the critical angle  $\theta_c=(2U_o/pv)^{1/2}$ , where  $U_o$  is the potential well depth,  $p$  and  $v$  the particle momentum and velocity, the particle is captured into the channeling regime and its trajectory oscillates between two adjacent planes. Channeled particles are deflected by the crystal bend angle. Channeling occurs also for bend radii  $R>R_c=pv/eE_m$  [2], where  $E_m$  is the maximum strength of the electric field of the crystal planes ( $E_m=6$  GV/cm for the main planes in Si), whilst the dechanneling probability increases with  $R$ . When using short crystals the dechanneling process is less frequent and the deflection efficiency increases. For instance, the 400 GeV/c protons of a quasi-parallel beam in the H8 line of the SPS North Area were deflected by a silicon crystal 2 mm long bent by 50  $\mu\text{rad}$  with efficiency larger than 83% [3], a value close to the theoretical limit of 86%.

The use of bent crystals for the beam extraction and for the halo collimation in circular accelerators was suggested in [4]. The extraction of 70 GeV/c protons with high efficiency, up

to 85%, was observed at IHEP U70 synchrotron [5]. The halo collimation assisted by a bent crystal was studied with the proton beam at the IHEP synchrotron, later with the gold nuclei beam at the RHIC [8], and with the 980 GeV/c proton beam at the FNAL [9]. In this case, the use of the crystal resulted in a factor two reduction of the background in the CDF apparatus.

The idea of UA9 is to test a collimation system assisted by short bent crystals in the CERN-SPS and to detect its efficiency, which is expected to increase due to the multiple passages of the circulating beam halo particles through the crystal [6, 7]. Simulations show that with a 2 mm long crystal bent by 150  $\mu$ rad the collimation efficiency should be of 99% whilst the crystal angular acceptance should become considerably larger than  $2\theta_c = 40\mu$ rad.

### **Scheme of UA9 experiment**

The UA9 experiment was approved in September 2008 and was operational as from June 2009. Its main goal is to demonstrate the feasibility of the crystal collimation using the SPS in storage mode as a test-bed to detect the efficiency. The strong point of UA9 is the very rich set of detectors installed close to the collimation devices. UA9 took data in six periods during 2009.

The experimental scheme of UA9 is shown in Fig.2. The collimation system is made of two stations whose relative phase advance is 90 degrees. The first station contains two bent crystals (CR I and CR II) alternatively used as primary collimators while the second is composed of a tungsten absorber 60 cm long (TAL). Both of them are installed at SPS azimuths with a large value of the horizontal beta function, upstream of the quadrupoles QF518 and QF520 respectively. The two silicon crystals are 2 mm long with the bend angle of about 150  $\mu$ rad. They are mounted in a tank on two in-vacuum goniometers. The crystal in the upstream position called CR I is a strip crystal [10] bent along the (110) equidistant planes. The other, called CR II, is a quasi mosaic crystal [11] bent along (111) non-equidistant planes (the channel width ratio is 3). The crystal orientation and horizontal position relative to the closed orbit are controlled by the two goniometers with high precision (2  $\mu$ rad for the angle and 5  $\mu$ m for the position). In the course of the year the angular precision and reproducibility was seriously deteriorated by mechanical damage of the goniometers.

In the tank of the primary collimators there are also a 2 mm long tungsten scatterer and an in-vacuum horizontally movable Cherenkov quartz detector I. This Cherenkov detector can be used to register either primary protons or secondary particles generated in the crystal. The scintillation telescope TEC3-TEC4 placed downstream the tank is used to monitor the

effect of inelastic interaction of protons. The GEM detectors installed upstream and downstream of the tank walls are used for the same purpose but they can also provide the angular distribution of the secondary particles produced in such interactions.

The TAL serves as secondary collimator and is placed in a tank upstream of the quadruple QF520, where the angular deflection acquired by particles in the crystal is transformed into a large horizontal displacement. The Cherenkov detector II mounted at the front wall of the TAL can register the protons deflected by the crystal before their absorption in the TAL. A MEDIPIX-type detector with  $256 \times 256$  square pixels is mounted in a Roman Pot 20 m upstream of the TAL. The MEDIPIX has a pixel size of  $55 \mu\text{m}$  and can register the spot of the halo deflected by the crystal. A LHC collimator prototype with two 1 m long graphite jaws is mounted about 1 m upstream the MEDIPIX.

### **SPS beam set-up and device alignment**

The crystal-assisted collimation was prepared using the following procedure. The SPS proton beam was accelerated and stored at 120 GeV/c. In most of the cases, the beam was made of a single bunch with few  $10^9$  up to  $10^{11}$  protons. Sometimes 12 bunches for a total population of  $10^{12}$  particles were stored. The diffusion speed was governed by the multiple scattering with the residual gas in the beam pipe. Occasionally a noise was injected into the transverse damper for a faster diffusion speed, however this method was quickly abandoned due to the difficulty to control the diffusive process itself. In most of the cases, when the crystal (or any other movable part of UA9) was positioned in the peripheral of the circulating beam, the beam lifetime was from a few up to 10 hours and the number of particles hitting the crystal (or the selected obstacle) from 10 to  $10^3$  protons per turn.

At the beginning of each run, the transverse RMS beam size  $\sigma_x$  was measured with a flying wire scanner and then the beam shape was cut at  $5-7 \sigma_x$  using the LHC collimator jaws. After that, all the movable objects of UA9 (crystals, TAL, scatterer and Cherenkov I) were put just at the edge of the LHC collimator shadow using the readings of the closest downstream BLM. This alignment procedure of the UA9 devices in each run allowed a very precise control of their mutual transverse positions.

### **Measurements with beam loss monitors**

The crystal collimation was made operational with the following procedure. The selected crystal was moved to its reference positions, say at  $6\sigma_{cr}$ . Then TAL was also moved at its reference position  $6\sigma_{tal} + x_{of}$ , where  $x_{of}$  was a 2-3 mm clearance. The size of the selected

clearance was such that particles not deflected by the crystal in channeling state at the first passage could miss the TAL and have supplementary chances of being channeled in the subsequent passages through the crystal. Finally the LHC collimator jaws, used to assist the alignment, were retracted to their garage positions and the angular scan of the crystal could start.

Fig.3 shows the dependence of the rate measured by the scintillation telescope TEC3-TEC4 as a function of crystal 1 orientation angle. The telescope counts are in general reduced by a factor five when the crystal planes are parallel to the beam envelope. In these conditions, the TAL promptly absorbs the deflected protons in less than a turn. The drop of the nuclear loss rate is explained as follow. Protons in well-channeled states move through the crystal far from the channel walls. They have no close collisions with the crystal nuclei. The nuclear inelastic interactions occur mainly for the small fraction of particles, which are non-channeled or de-channeled. The angular range with reduced counts to the right of the channeling peak is due to volume reflection (VR) of protons from bent planes in the crystal. The length of the volume reflection plateau is about equal to the crystal bent angle. Protons deflected by an angle about  $\theta_c$  due to VR can pass a few times through the crystal before they hit the TAL. However, the number of passages is considerably smaller than for amorphous orientations of the crystal. This explains the drop of the counting rate in the VR plateau.

By performing a wide range angular scan with crystal 1, several angular ranges with peaks of channeling and VR were found. This behavior is eventually induced by an orientation of the crystal with respect to the beam envelope rather close to the  $\langle 111 \rangle$  axis direction. Channeling and VR will appear whenever the beam envelope is almost parallel to one of the skew planes passing through the  $\langle 111 \rangle$  axis. The skew planes effect was to some extent very interesting to be studied, but was inducing unwanted features in the extracted beam: they can be easily avoided by a proper crystal inclination during the installation.

### **Measurements with LHC collimator scan**

Once the crystal orientation was optimal for the deflection of halo protons into the TAL, the LHC collimator was used to perform a horizontal scan of the deflected beam. The LHC collimator was slowly displaced from the garage position up to the closed orbit, thereby intercepting the trajectory of the deflected beam. The collisions of the protons with the collimator produced secondary fragments, which were registered by BLM 1 and 2 located downstream the LHC collimator.

Fig.4a shows the BLM count rate as a function of the LHC collimator position. The count is proportional to the number of protons interacting with the collimator. The BLM count increases fast from left to right when the collimator intersects the beam fraction deflected by the crystal. Then the count rate increases very slowly up to the position where a very sharp increase indicates that the circulating beam core is intercepted Fig.4b shows the numerical derivative of the BLM count rate, which reproduces the deflected beam shape. The beam deflected by the crystal is shifted from the circulating beam by about 5 mm at the LHC collimator position.

The scans with the LHC collimator had been performed with both crystals. The best values of the collimation efficiency estimated from these measurements for the crystal 1 and 2 are 74% and 77.4%, respectively. The different deflection angles observed in these measurements are explained by the different angular positions of the crystal realized with the goniometer near the perfect alignment. Indeed the proton deflection angle is the sum of the crystal bend angle and of its inclination angle with respect to the beam envelope.

### **Measurements with MEDIPIX detector**

Measurements of the beam halo deflected by the crystal were also performed with the MEDIPIX detector. Fig.5a shows the two-dimensional distribution of the deflected beam fraction. Fig.5b shows the horizontal projection of the distribution. The distribution peak position corresponds to the particles deflected by the crystal bend angle. The tail on the right is due to dechanneled particles. The level of the detector background corresponds to the plateau on the left of the peak. Once the background is subtracted, the number of events registered by the MEDIPIX gives the number of deflected protons. The number of halo particles, which hit the crystal, was determined by the measurements with the Beam Current Transformer (BCT). The collimation efficiency defined as the ratio of the deflected protons registered with the MEDIPIX to the proton number hit the crystal was about 86% in the last data-taking session, with a large error of about 18% due to the low sensitivity of BCT and to the calibration procedure of the MEDIPIX.

### **Measurements with TIDP scan**

An estimate of the leakage of the crystal collimation setup was made in the following manner. The transverse region surrounding the circulating beam was scanned using a collimator (TIDP) located in the octant 1 of the SPS close to QF114 in a position with large horizontal beta-function and large dispersion. The presence of particles circulating far from

the beam core, above  $6\sigma_x$  was associated to the counting rate of the BLM 114 downstream the TIDP. A counting rate above the threshold was recorded only between  $6\sigma_x$  and  $8\sigma_x$ . This rate is due to the small fraction of protons scattered in the crystal. In our interpretation these particles have a large probability of being channeled and deflected by the crystal in the subsequent turns. In the limit of the BLM sensitivity we were unable to detect particles at large amplitude above  $8\sigma_x$ . This observation is an additional confirmation of the fact that the collimation efficiency with the crystal is very high. Indeed, the inefficiency should be determined only by the nuclear interactions of protons in the crystal, which are strongly suppressed by the alignment of crystal in channeling mode.

## **Conclusions**

The UA9 studies performed with bent crystals in the SPS during the six runs of 2009 bring us to the following conclusions.

1. The optimal crystal alignment for halo particle deflection in channeling mode is fast and well reproducible. It can be based either on beam loss detectors or on the direct observation of the deflected beam with the MEDIPIX detector.
2. Estimates of the collimation efficiency performed with the LHC prototype collimator scan or with the direct observation of the deflected beam with MEDIPIX range from 60% to 99%. Such a large fluctuation is due to the uncertainty induced by the low-sensitivity of the Beam Current Transformer, by the calibration of the loss rate versus beam intensity and by the calibration of MEDIPIX in counting mode.
3. The measurements with the scraper (TIDP) scan show no sign of leakage of the collimation. The collimation efficiency should be close to 100%.
4. The BLM near the crystal show that the nuclear loss rate for the aligned crystal is reduced five times with respect to the amorphous orientation.

## **Suggestions for the future studies**

1. Install the IHEP goniometer, which should have a better reproducibility. It allows mounting two new crystals with smaller parasitic curvatures. This fact may considerably help the crystal collimation procedure.
2. Equip a new station in the high-dispersion area upstream the quadruple QF522, which should register a possible leakage of the crystal collimation. This station will be equipped

with a new Roman Pot including a MEDIPIX, with a new Cherenkov detector and stopper. This allows a straight registration of the leakage protons.

3. Prepare and test the crystals in the North Area for the next experimental campaign in the SPS and later the installation in the LHC.

## References

- [1] J. Lindhard, K. Dan. Vidensk. Selsk. Mat. Fys. Medd. 34 (1965) 14.
- [2] E.N. Tsyganov, Preprint TM-682, TM-684, Fermilab, Batavia (1976).
- [3] W.Scandale et al., Phys. Letters B 680 (2009) 129.
- [4] V.M.Biryukov, V.N.Chepegin, Yu.A.Chesnokov, V.Guidi, W.Scandale, Nucl.Instr.Meth.B 234 (2005) 23.
- [5] A.G.Afonin et al., Phys.Rev.Letters 87 (2001) 094802.
- [6] A.M.Taratin, S.A.Vorobiev, M.D.Bavizhev, I.A.Yazynin, Nucl.Instr.Meth.B 58 (1991) 103.
- [7] V.M.Biryukov, Nucl.Instr.Meth.B 58 (1991) 202.
- [8] R.P.Fliller et al., Nucl.Instr.Meth.B 234 (2005) 47.
- [9] R.A.Carrigan Jr. et al., Fermilab-CONF-06-309-AD.
- [10] S. Baricordi, et al., Appl. Phys. Lett. 91 (2007) 061908;  
S. Baricordi, et al., J. Phys. D: Appl. Phys. 41 (2008) 245501.
- [11] Yu.M.Ivanov, A.A.Petrunin, V.V.Skorobogatov, JETP Letters 81 (2005) 99.

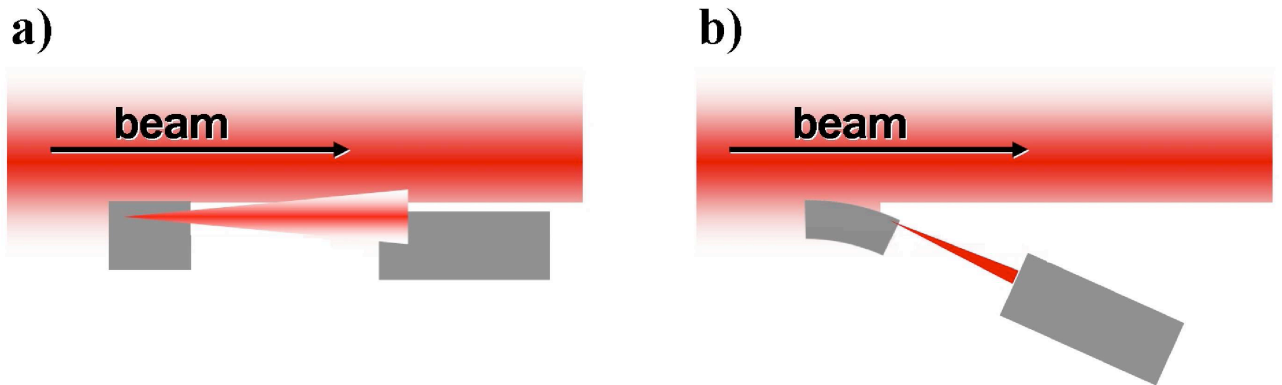


Fig.1. a) Collimation using a solid state primary collimator-scatterer. b) Collimation with a bent crystal as a primary collimator. Halo particles are deflected and directed on the absorber far from its edge.



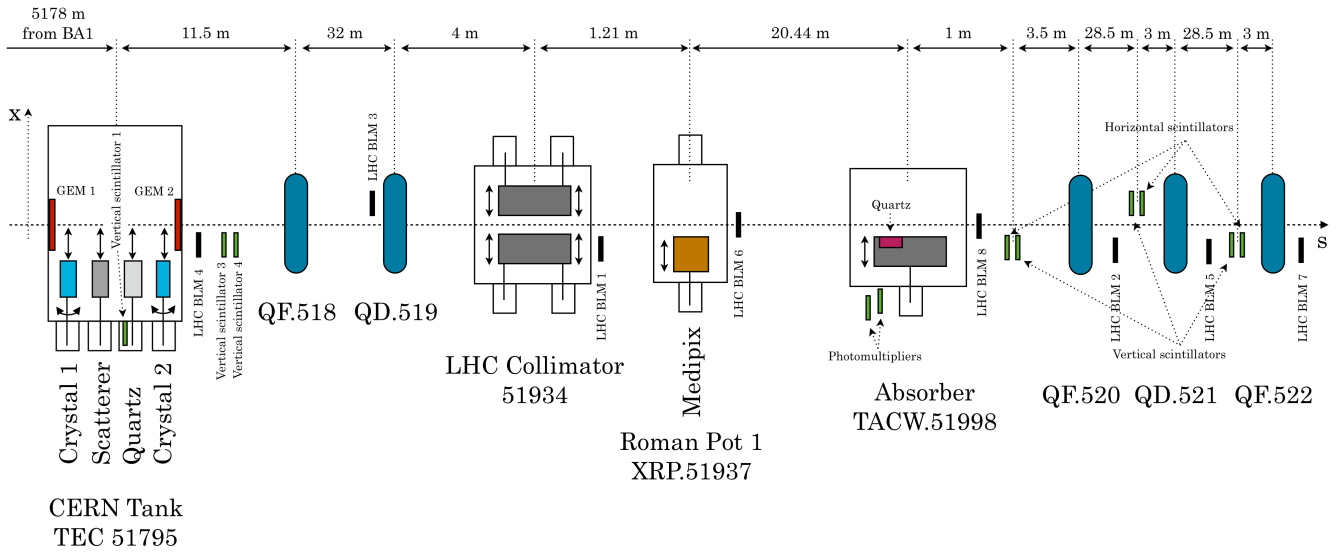


Fig.2. The UA9 experimental layout. The primary collimators – bent crystals I and II are located upstream the quadrupole QF518. The TAL acting as secondary collimator (Absorber) is upstream the quadrupole QF 520.

### Scan Crystal 1 Jul 1st

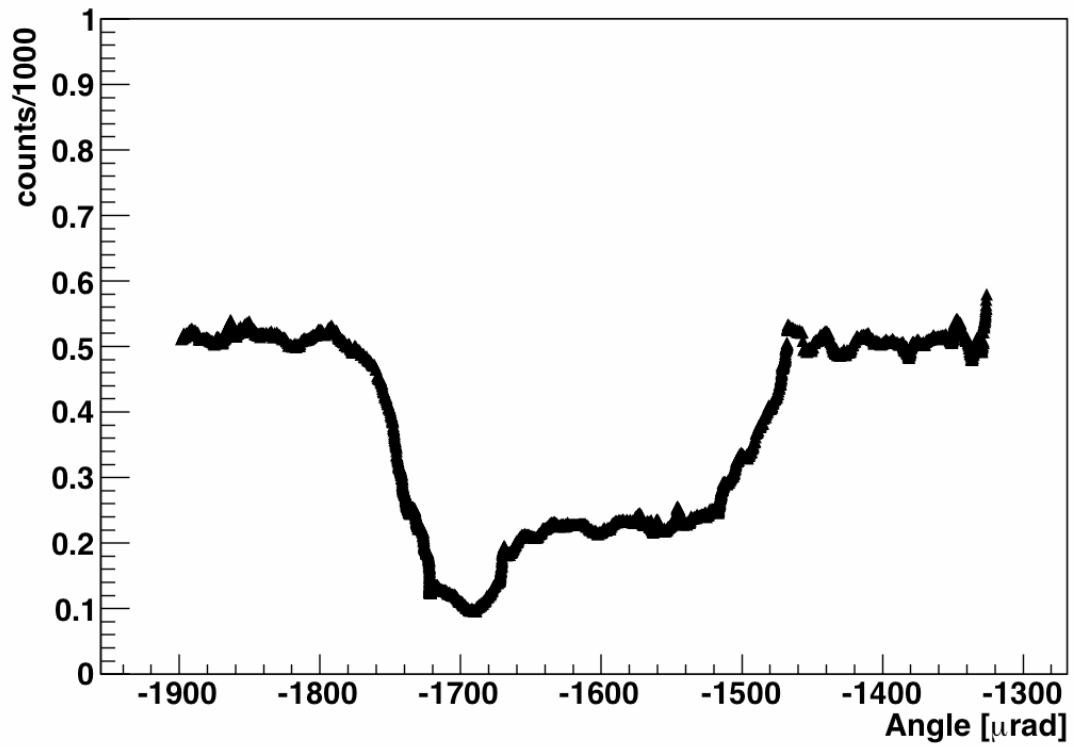


Fig.3. Dependence of inelastic interaction losses of the SPS halo protons in the crystal primary collimator versus its orientation angle. The minimum at about -1700  $\mu\text{rad}$  is due to channeling of protons, which are deflected and directed to the absorber.

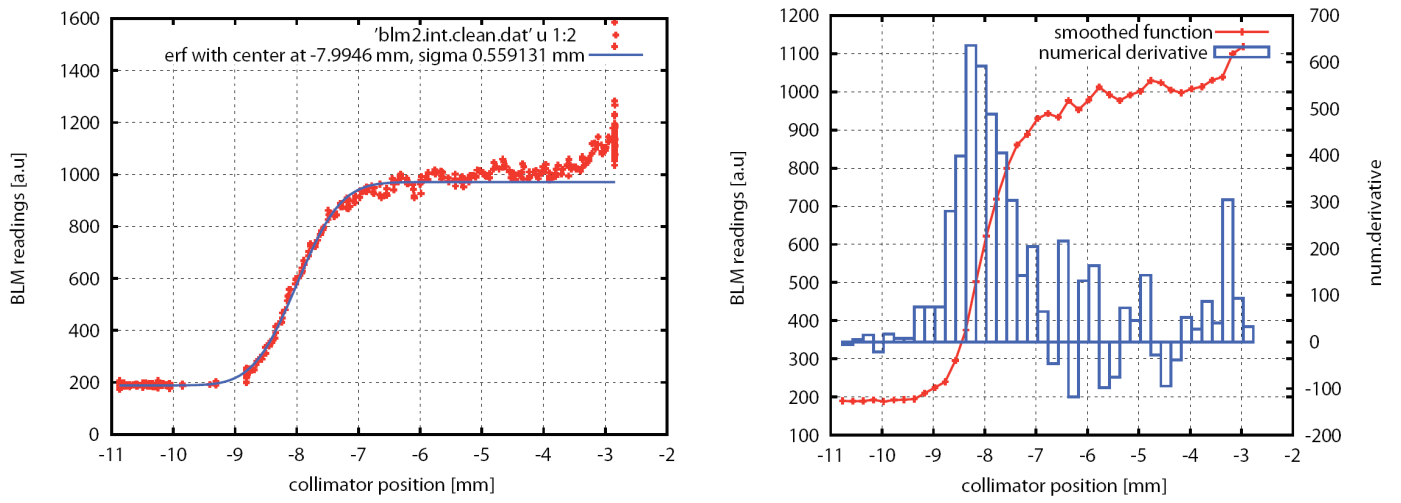


Fig.4. Intersection of the beam deflected by the crystal with the LHC prototype collimator. a) dependence of the BLM count on the horizontal position of the LHC collimator during its scan towards the closed orbits position. b) the numerical derivative of this dependence, which shows the shape of the deflected beam with its center near -8 mm.

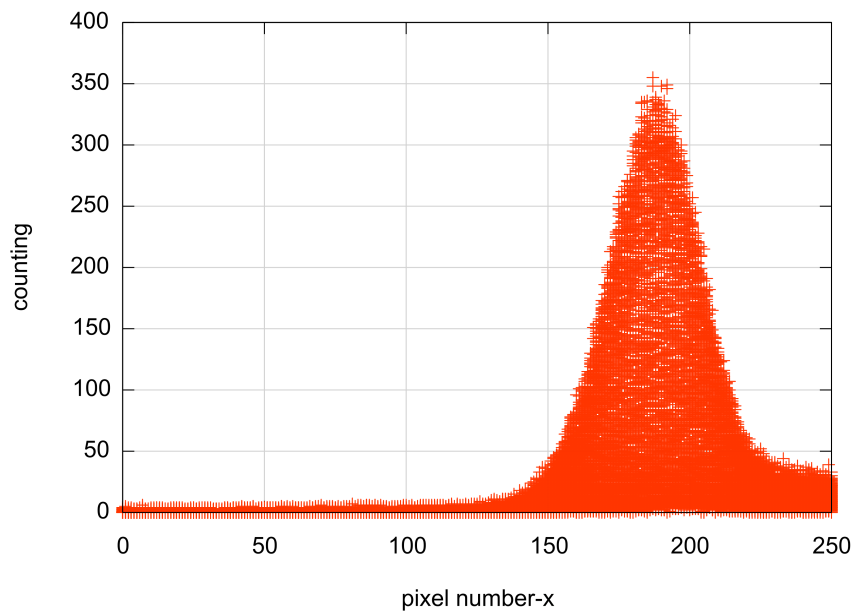
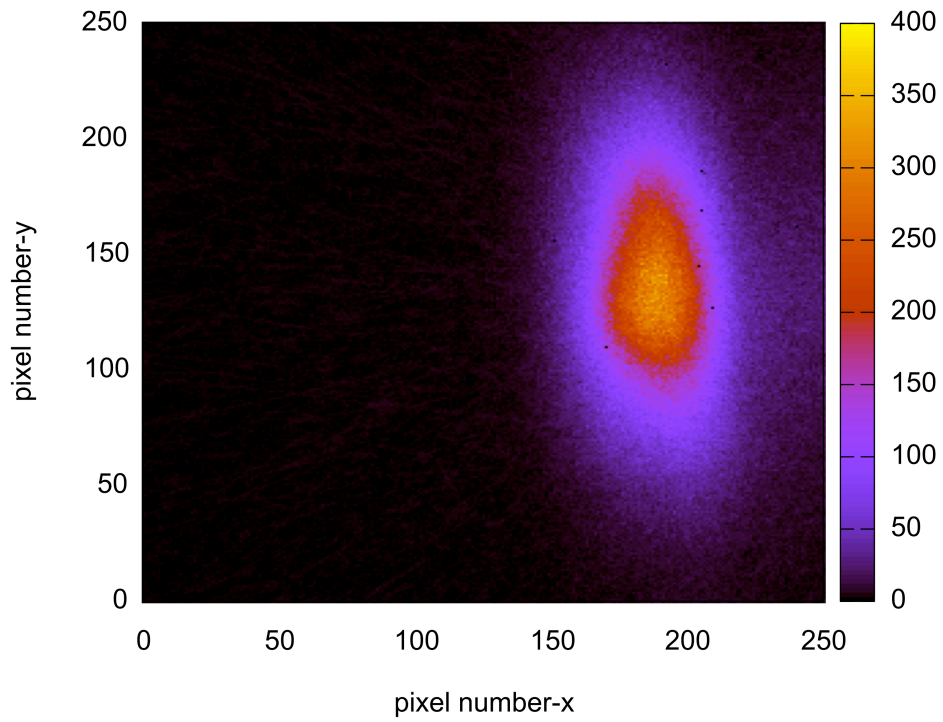


Fig.5. a) Image of the SPS halo deflected with the crystal obtained with the MEDIPIX detector, b) its horizontal projection integrated over a tiny y-slice around the extracted peak. The maximum is due to protons deflected by the full bend angle, the shoulder on the right is the tail of dechanneled particles.

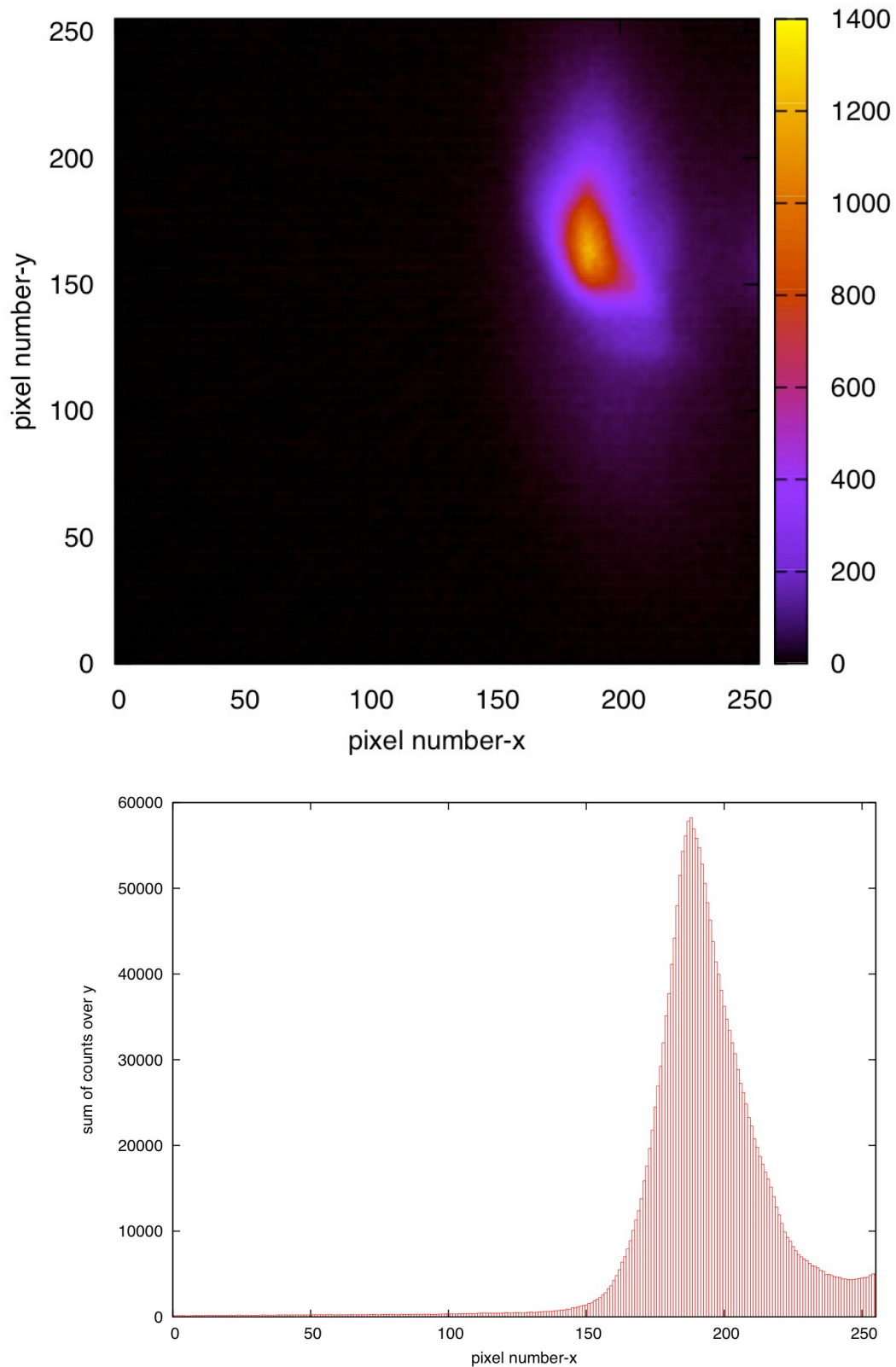


Fig.6. a) Image of the SPS halo deflected with the crystal obtained with the MEDIPIX detector, b) its horizontal projection integrated over the extracted peak. The maximum is due to protons deflected by the full bend angle, the shoulder on the right is the tail of dechanneled particles.

